



PHOTOELASTIC ANALYSIS OF DRY LINE CONTACT PROBLEM

UNDER COMBINED LOADING

SH. EL KORDY**

A. EL SANABARY*

N. GADALLAH*

ABSTRACT:

This study concerns the photoelastic analysis of dry contact between a cylinder and a plane under combined loading. Both static and dynamic cases are experimentally dealt with. A test rig is specially designed to collect essential data within and in the vicinity of the contact area.

Data obtained have been analysed to estimate the contact area, normal and tangential stress distributions, coefficient of friction and the position of maximum shear through the contact. Results are compared with theoretical and experimental values (previously published) by other authors.

The comparison of dynamic with static experimental results clarifies the angle of asymmetry of maximum shear stress fringes corresponding to the angle of friction.

INTRODUCTION

The modified adhesion theory [1] was established on the basis of plastic deformation of the higher asperities in contact withstanding applied loads. Different analysis [2,3,4] showed a contribution of the elastic deformation to the deformation mechanism, and consequently the way a contact transits from elastic to elastoplastic contact mode. The friction is influenced by these modes, which contribute to the balance of energy loss at the contact, that is as long as plastic deformations are constrained a reduction in the energy loss is expected.

On this basis, the contact area is investigated and evaluated in both static and dynamic cases. Results are compared with hertzian contact, and those after the modified adhesion theory [3,6].

* Lecturers, M.T.C, Kobry EL Kobba, Cairo-EGYPT

**M.Sc.Mech.Eng., M.T.C.

A mesh analysis is introduced to handle the photoelastic data, and a stress analysis of a line contact after [3] is presented which conforms with the obtained results.

TEST RIG AND MODES OF OPERATION:

A cylinder-plane contact is modelled by a PSM-5 photoelastic material (Fig.1) of fringe value 60 psi/fr/inch, stress-optic coefficient $K=240$ psi/fr (1.65 MPa/fr), and Young's modulus $E=150$ MPa.

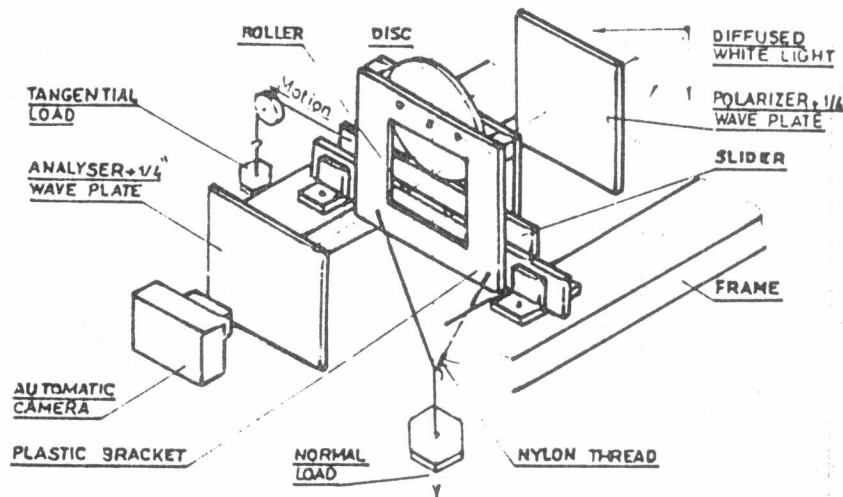


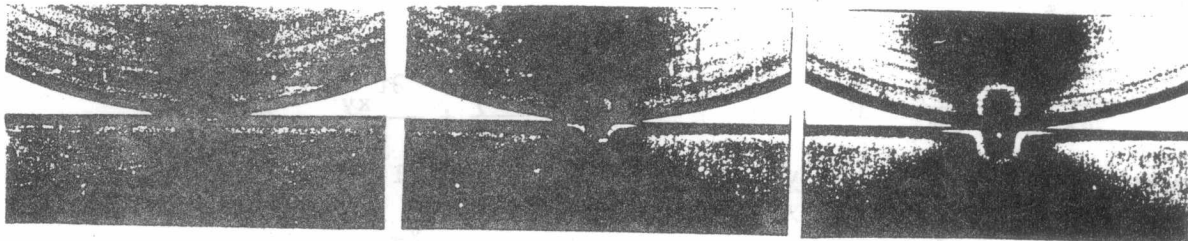
Fig. EXPERIMENTAL TEST RIG.

Static normal loads ranging from 10-50 N are applied. With each load a tangential force is increasingly applied until relative motion starts. A coloured photograph of the contact withstanding only normal load is taken. A second photo is taken at the instant where relative motion starts. The coloured isocromatic patterns are analysed at fringe orders of half wave length of a bright set-up condition, table (1) . The calibrating table of white diffused light [7] is hereby adapted. The shear stresses corresponding to different fringe colours are then depicted. The loading patterns for selected loads of 10,30 and 50 N are shown in (Fig.2).

A complete stress analysis in static and dynamic cases at 50 N normal load is presented hereafter .

Table 1 . Visible colours and equivalent maximum shear stress.

Order	Visible colour	Relative retardation λ'	$2 \tau_{max}$ MPa
1/2	Orange	2525	0.5618
1/2	Red	2680	0.7491
1/2	Black	-	0.825
1/2	Blue green	3320	1.237
1	White	3935	1.650
1	Yellow	4450	1.903
1	Red	4990	2.092
1	Yellow white	5340	2.239
1	Green blue	6290	2.638
3/2	Clear yellow	6825	2.862
3/2	Red	8040	3.371

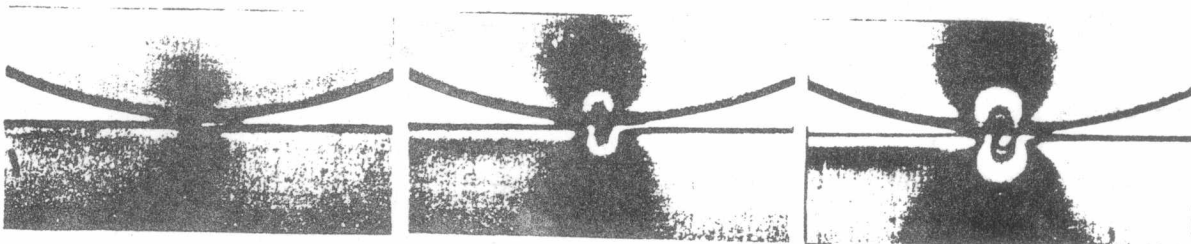


w= 10N

w = 30N

w= 50N

a) Normal Load.



w= 10N , T= 3.43 N

w=30N, T=4.41N

w= 50N, T=3.14N

b) Normal and tangential load.

Fig.2. ISOCAROMATIC PATTERN.

MATHEMATICAL FORMULATION AND MESH ANALYSIS

The isochromatic pattern obtained is enlarged to a scale 40 :1. The isochromatic pattern comprises 10 fringes, each is divided to 18 nodes (Fig.3). The directional angle (ψ) at any point on an isochromatic fringe represents the direction of the max shear stress at the same point. Angle ψ may be approximated as

$$\tan \psi = \frac{R_2 \sin \theta_2 - R_1 \sin \theta_1}{R_2 \cos \theta_2 - R_1 \cos \theta_1}$$

Thus, the directional angle (ϕ) of the principal stress σ_1 is found as

$$\phi = \psi - 45^\circ$$

From the theory of strength and Mohr's analysis [7]

$$\tau_{xy} = 0.5 (\sigma_1 - \sigma_2) \sin 2\phi = \tau_{\max} \sin 2\phi$$

The element equilibrium equation in a biaxial state of stress can be written as :

$$\frac{\partial \sigma_x}{\partial x} + \frac{\partial \tau_{xy}}{\partial y} = 0 \quad ; \quad \frac{\partial \sigma_y}{\partial y} + \frac{\partial \tau_{xy}}{\partial x} = 0$$

$$\text{Thus: } \sigma_{x1} = \sigma_{x0} - \int_{x_0}^{x1} \left(\frac{\partial \tau_{yx}}{\partial y} \right) dx \quad ; \quad \sigma_{y1} = \sigma_{y0} - \int_{y_0}^{y1} \left(\frac{\partial \tau_{xy}}{\partial x} \right) dy$$

Using finite difference approximation, with $\Delta x = \Delta y$ yields:

$$\frac{\Delta \sigma_x}{\Delta x} = - \frac{\Delta \tau_{yx}}{\Delta y} \quad \text{or} \quad \Delta \sigma_x = \Delta \tau_{yx} \quad \text{and} \quad \Delta \sigma_y = -\Delta \tau_{xy}$$

From which

$$\sigma_{x1} = \sigma_{x0} - \sum_0^1 \Delta \tau_{yx} \quad , \quad \sigma_{y1} = \sigma_{y0} - \sum_0^1 \Delta \tau_{xy}$$

Thus σ_x distribution is obtained through the continuous integration over a specific line. According to the maximum shear theory of a failure after Tresca [2].

$$\sigma_1 - \sigma_2 = S = | (\sigma_x - \sigma_y)^2 + 4 \tau_{xy}^2 |^{1/2} = 2 \tau_{\max}$$

$$\sigma_y = \sigma_x - (S^2 - 4 \tau_{xy}^2)^{1/2}$$

where S is the data depicted from the fringe pattern in N/mm^2 .

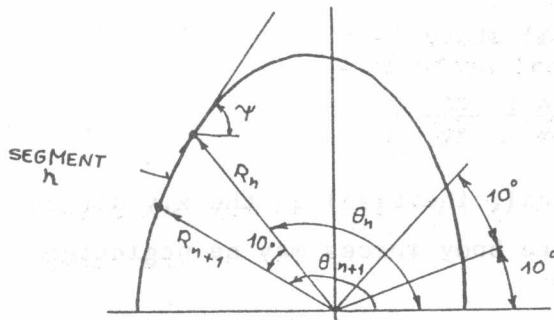


Fig.3. Mesh Convention.

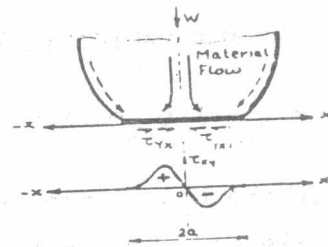


Fig.4. A curved to flat contact.

STRESS ANALYSIS OF LINE CONTACT IN COMBINED LOADING

At contact boundaries where material flow is not prevented to relax under normal loading a sort of slip is generally experienced [4,5]. This slip clearly appears in the case of curved to flat contacts (Fig.4). If (f) is the coulomb coefficient of friction, and p(x) is normal load distribution at the contact then the frictional traction T is

$$T = \int_{-a}^a f \cdot p(x) dx = \int_{-a}^a t(x) dx$$

where a is the semicontact width. Therefore the intensity of traction $t(x)$ follows the normal load distribution p(x), (Fig.5).

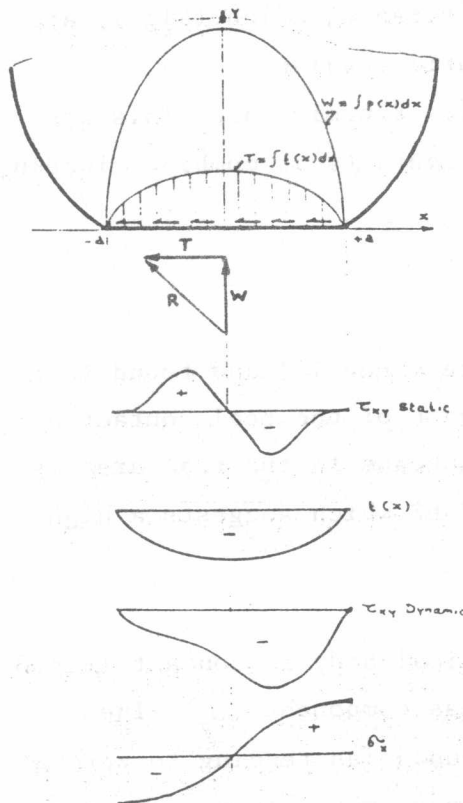


Fig.5. Combined Load effect

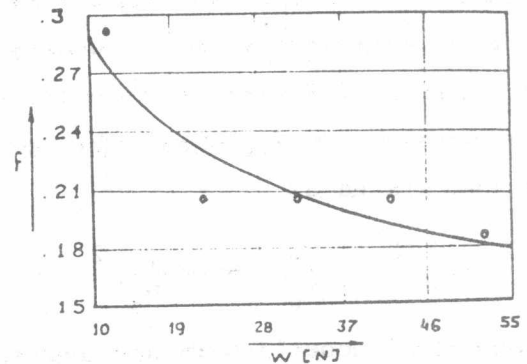


Fig.6. Coeff. of friction with normal load.

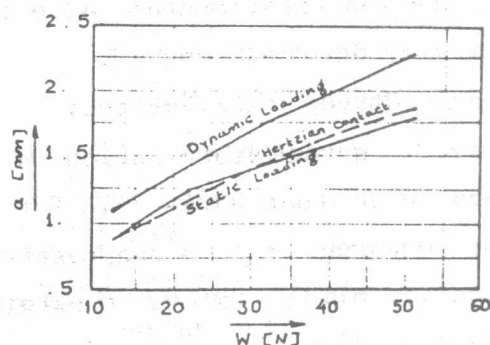


Fig.7. Contact area

The compatibility equation in bidimensional state is :

$$\left(\frac{\partial}{\partial x^2} + \frac{\partial}{\partial y^2} \right) (\sigma_x + \sigma_y) = -(1+\nu) \left(\frac{\partial X}{\partial x} + \frac{\partial Y}{\partial y} \right)$$

where X,Y are the body forces (gravitational, inertial) in the x,y directions respectively . For small masses where body forces may be neglected $\nabla^2 = 0$

It is seen. that the equation is material independent, therefore contacts of similar geometries and load distributions would have the same distribution of stress [7].

DISCUSSION OF RESULTS

1. Friction Coefficient:

The values obtained for the dynamic coefficient of friction, (Fig.6) are regressed with a correlation coefficient $R=0.996$ to the relation:

$f=0.287 (w)^{-0.283}$, this means $T=0;287(w)^{0.717}$, where the exponent (0.717) is reasonable, the practical range being (0.66 upto 1) in soft solids [10]

The static coefficient of friction has been evaluated as $\frac{\int \tau_{xy}(x)}{\int \sigma_y(x)}$ over the contact, giving an average of 0.387.

2. Apparent Contact Area:

values of theoretical areas obtained from hertzian equation (Fig.7) are in good agreement with calculated areas at static loading.

An increase of 22-28% at (10-50)N is observed in dynamic case. This was confirmed by [6,9], where the area of plastic contacts at combined loading is calculated as

$$(A_r)^2 = \left(\frac{W}{p_o}\right)^2 + \alpha \left(\frac{T}{p_o}\right)^2 \quad ; \quad T = f.W.$$

where the α coefficient was experimentally determined [1] and found to be 9. An increase of $9f^2$ was detected for the square of the real contact areas. At high loads reaching 50 N, the calculated increase in the real area is 14.8%, and the experimental value indicates 28.6% which suggests a high plastically deformed contact.

3. Static Stress Distributions:

The static stress distribution in the cylindrical body in contact (Fig.8) conforms with other works [11] for normal stress component (σ_y). The stress component (σ_x) is compressive at the boundaries tending to zero at the contact middle. Values of obtained τ_{xy} support the slip phenomena as reported in [5,9].

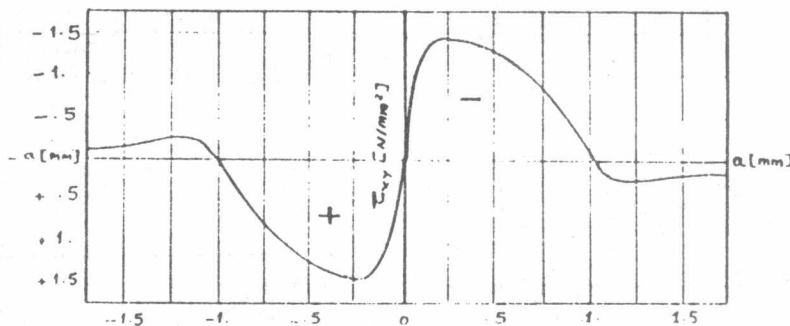
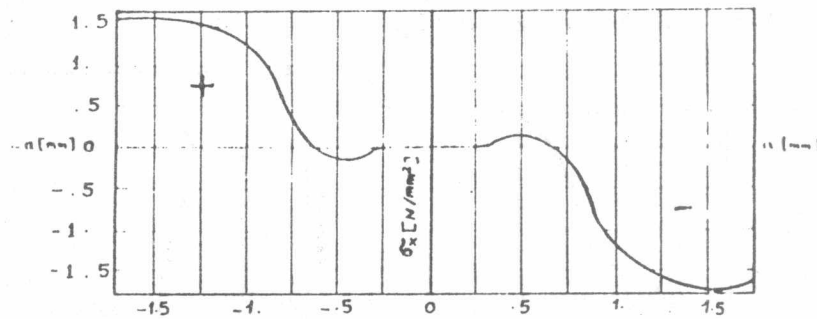
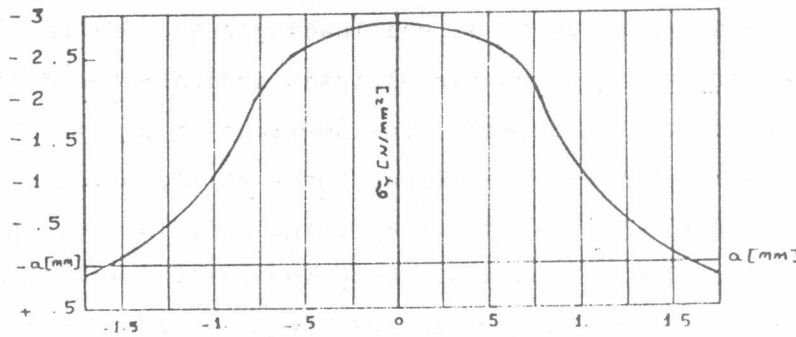


Fig.8. Stress distributions under normal load.

4. Plastic Onset :

The point of plastic onset is located at a distance $0.428a$ (Fig.9) measured from contact surface, ($a..$ being the semicontact width). Publications for hard metals [4,9,12] and polymers [13,14] suggest a dependance on poisson's ratio ν . For most polymers ($\nu=0.5$), a depth of $0.533 a$ had been reported. In a two dimensional case, as considered in this work, where load friction favours plastic deformation [4], the authors find the results reasonable.

5. Dynamic Stress Distribution:

Normal and tangential loads evaluated from the areas under the curves

$\sigma_y(x)$ & $\tau_{xy}(x)$ (Fig.10) were found to be 48.59 and 9.3 N respectively. Consequently, relative error to actual loading are 2.82% and 1.4%.

The axis of symmetry of isochromatic ellipses indicate the direction of the resultant force at the centroid. The smallest fringe is considered the most representative to the resultant force at midcontact. The slope of this direction with the y-axis is 0.176, (Fig. 11). The average value of the friction coefficient obtained experimentally ($f=0.183$). The relative error is -3.67%. Proceeding away from the contact (larger fringes) results in decreasing the angle to zero at approximately a depth equivalent to contact width (fig. 12).

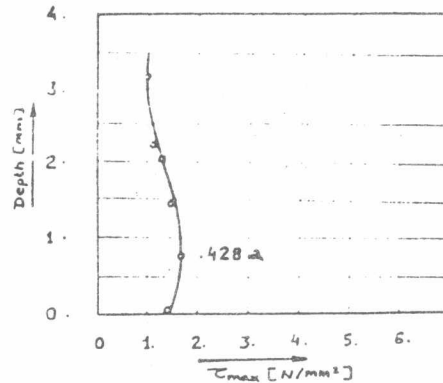
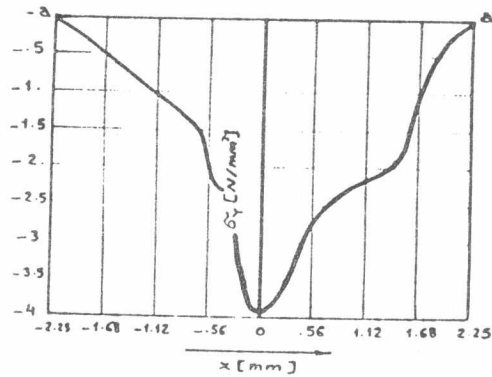


Fig.9. Plastic Onset Position

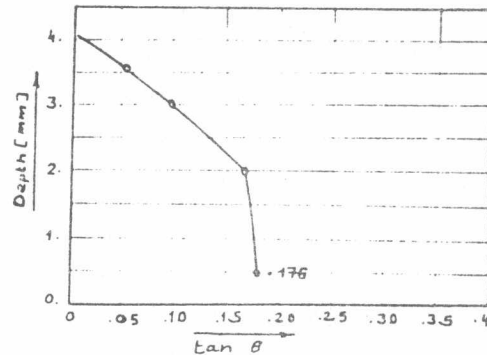
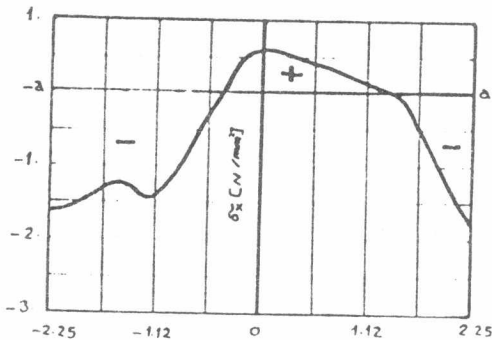


Fig.11. Angle of asymmetry.

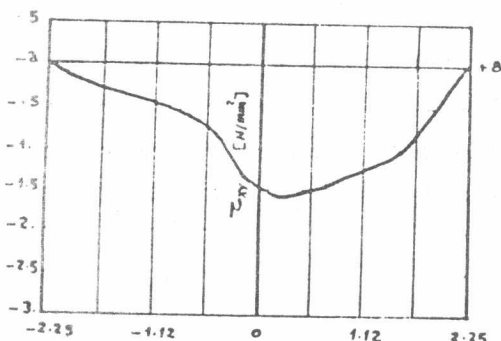


Fig.10. Stress distribution under combined.

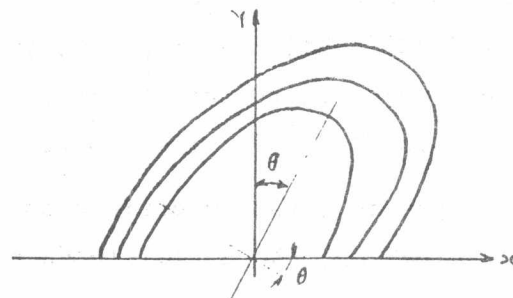


Fig.12. Fringe pattern under combined loading.



CONCLUSION

The simple laboratory device is used to simulate a line contact in normal and combined loading with relative motion. The following remarks have been observed:

1. The dynamic coefficient of friction is decreased with increasing normal load.
2. In static loading, the contact area exhibits more conformity to the theoretical hertzian contact, yet this is not observed with combined loading.
3. Two aspects of frictional tractions are quietly observed; the increase in the peak pressure, and the very small influence on the stress distributions which does not exceed the contact width.
4. Plastic onset results a concentration factor of 1.17 following the shear theory of failure, and closer to the interface due to the frictional tractions in the static case.
5. The axis of symmetry of isochromatic fringe ellipses at the contact middle is of two valuable indications; the friction angle and the small influence of traction friction away from the contact.

REFERENCES:

- (1) BOWDEN, F.P., and TABOR, D., "Friction and lubrication of solids", Oxford Univ. Press, Part I, 1954-Part II, 1964.
- (2) BUSSHAN, B., "Analysis of the real area of contact between Polymeric magnetic medium and a rigid surface", Jour. of Trib. Vol. 106, 1984
- (3) EDWARDS, C. M., and HALLING, J., "An analysis of the plastic interaction of surface asperities and its relevance to the value of coefficient of friction", Jour. of Mech. Eng. Science, 10, 1968, P.101.
- (4) NAGARAJ, H.S., "Elastoplastic contact of bodies with friction under normal and tangential loading", Jour of Trib, Vol. 106, PP.519-626.
- (5) SALAMON, N.J., and MAHMOUD, F.F., "Effects of profile roughness and Friction in contacting bodies in compression", wear, Vol. 101, 1985, PP 205-218 .
- (6) MOORE, D.F., "Friction of metals-principles & Application of Tribology" ed . Moore, Pergamon press, 1975, PP. 33-59.
- (7) KUSKE, A., and ROBERTSON, G., "Photoelastic-stress analysis", eds. Kuake ; A., and Robertson, G., John Willey and sons, London, 1974.



- (8) MOORE, G., "Continuum mechanics", Schaun's Series, e.d. Mase, G., McGraw-Hill, 1970, PP. 175-194.
- (9) HALLING, J. and NURI, K.A., "Contact of surfaces-Principles of Tribology", ed Halling, the MacMillan Press, 1975, PP. 40-67.
- (10) RABIN OWICZ, E., "Dry friction -Standard Handbook of Lubrication Engineering", eds. O'connor and Boyd, 1968, pp.1-26.
- (11) DUNDERS, J. TSAI, K., and KEER, L., "Contact between elastic bodies with wavy surfaces", Jour. of Elast., 3, 1973, pp.105-119.
- (12) GOODMAN, L.E., "Contact stress analysis of normally loaded rough spheres", ASME, Jour. of App. Mech., Vol. 84, 1962, pp. 515-522.
- (13) DAVIE S, R.M. "The determination of static and dynamic yield stresses using steel balls", Proc. Roy. Soc. London, Vol. A197, 1949, pp.416-432.
- (14) SHOM, M.C., and DS SALVO, G.J., "A new approach to plasticity and its application to blunt two dimensional indenters", ASME, Jour. of Eng. For Industry, Vol. 37, 1970, pp. 429-479.